Accepted Manuscript

The axisymmetric shrink fit problem subjected to axial force

J.P. Lopes, D.A. Hills, R.J.H. Paynter

PII: S0997-7538(17)30928-2

DOI: 10.1016/j.euromechsol.2018.02.007

Reference: EJMSOL 3550

To appear in: *European Journal of Mechanics / A Solids*

Received Date: 13 December 2017

Revised Date: 8 February 2018

Accepted Date: 9 February 2018

Please cite this article as: Lopes, J.P., Hills, D.A., Paynter, R.J.H., The axisymmetric shrink fit problem subjected to axial force, *European Journal of Mechanics / A Solids* (2018), doi: 10.1016/j.euromechsol.2018.02.007.

The Axisymmetric Shrink Fit Problem Subjected to Axial Force

J.P. Lopes, D.A. Hills, R.J.H. Paynter

Department of Engineering Science, University of Oxford

Highlights

- A shaft-hub system is assembled under shrink-fit
- The assembly is modelled as a semi-infinite shaft embedded within an elastic half-space
- A bilateral solution is obtained under the assumption of no-slip
- The stress fields are corrected using glide ring dislocations
- The corrected solution is extended to a finite shaft

The Axisymmetric Shrink Fit Problem Subjected to Axial Force

J.P. Lopes[a,*], D.A. Hills[a], R.J.H. Paynter[a]

[a]*Department of Engineering Science, University of Oxford, Parks Road, Oxford OX1 3PJ, United Kingdom*

Abstract

A solution for the stress fields in a shaft-hub shrink-fit assembly subjected to an axial force is presented. The assembly is modelled as a semi-infinite shaft embedded within an elastic half-space. The stress field for a bilateral solution is obtained, considering that the contact interface is everywhere subjected to pressure and that the coefficient of friction is sufficient to prevent slip everywhere. This solution is then corrected to satisfy the slip condition using an array of strain nuclei in the form of glide ring dislocations. The contact pressure, shear traction and their ratio is presented as a function of the coefficient of friction and the ratio of shrink-fit to axial force stresses. Finally, the solution is extended to a finite shaft.

Keywords: Ring dislocations, Axisymmetric, Shrink Fit, Contact

1. Introduction

The classical solution for the contact pressure induced in an axisymmetric shrink fit problem is the well-know Lamé solution [1]. It is normally used in plane strain, and represents a very satisfactory solution at interior points well away from the edges, i.e. when $z \gg a$, Figure 1, where a is the radius of the shaft, and when the outer radius of the 'hub' (the part incorporating the hole) is much greater than the radius of the shaft, which is often at least approximately true. The question arises of how that pressure should be modified at the point of insertion of the shaft into the hub, and where the shaft and hub terminate. The latter problem was solved in closed form [2] providing a true local three dimensional correction for the presence of the free surface, and here we enquire how such an assembly responds to the application of a normal force (Figure 1) tending either to push the central shaft in, as shown, or tending to pull it out. In practice the details of the solution will depend, of course, on how the loading is distributed across the end of the shaft but providing that the points we are considering are not too close the details will not matter.

The general idea will be first to use the bilateral solution, that is one where we assume that the interface between shaft and socket is everywhere subjected to pressure and that the coefficient of friction is sufficient to prevent slip everywhere, so that the presence of the interface is not 'felt'. We will then probe the limits of this assumption, and go on to consider problems where a slip zone of finite extent develops by deploying distributions of circular glide dislocations to represent the effects of slip.

2. Adhered Solution

The geometry of the problem is shown in Figure 1. Upon assembly, an infinitely long shaft of radius $a + \Delta_0$ is inserted in a hub with a cylindrical hole of radius a, present in an elastic half-space. Both the shaft and the hub have Poisson's ratio ν and Young's modulus E. The assembly can be thought as inserting a shaft of radius a into a hole of same size under isothermal conditions and then heating only the shaft through a temperature differential ΔT, or by cooling the oversized shaft until it fits and then letting it warm back up. This results in an induced radial strain ϵ^* in the shaft, given by

$$\epsilon^* = \frac{\Delta_0}{a} = \alpha \Delta T \tag{1}$$

where α is the coefficient of thermal expansion for the shaft.

If the coefficient of friction is sufficiently high to prevent any slip, the state of stress that arises from this shrink-fit assembly is given by Paynter et al [2], and the stresses σ_{ij}^{SF} in a point (r,z), $z \geq 0$, are given by

*Corresponding author

Email addresses: jhonatan.dapontelopes@eng.ox.ac.uk (J.P. Lopes), david.hills@eng.ox.ac.uk (D.A. Hills), robert.paynter@eng.ox.ac.uk (R.J.H. Paynter)

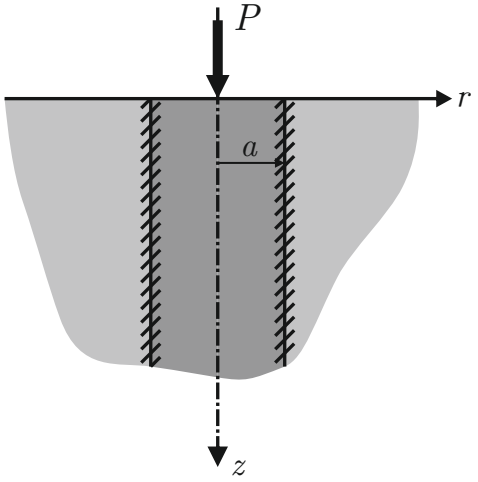

Figure 1: A semi infinite shaft of radius a in a half-space $z > 0$.

$$\sigma_{rr}^{SF}(r,z) = \sigma_0 \left[a\Big(J_{1,0;0} - z\, J_{1,0;1} + \frac{z}{r}\, J_{1,1;0} - \frac{\kappa - 1}{2r}\, J_{1,1;-1} \Big) + \begin{cases} -1/2 & r \le a \\ -a^2/(2\,r^2) & r > a \end{cases} \right] \tag{2}$$

$$\sigma_{zz}^{SF}(r,z) = \sigma_0\, a\Big(J_{1,0;0} + z\, J_{1,0;1} \Big) - \Big\{ \sigma_0 \quad r \le a \tag{3}$$

$$\sigma_{rz}^{SF}(r,z) = \sigma_0\, a\, z\, J_{1,1;1} \tag{4}$$

where $\sigma_0 = E\,\epsilon^*/(1-\nu)$ is the reference axial stress and $J_{m,n;p}$ are Lipschitz-Hankel integrals, defined in Appendix A.

The third kind elliptic integrals present in the Lipschitz-Hankel integrals in Equations (2) and (4) are singular when $(r,z) = (a,0)$. For this point, we obtain the stress values by taking the limit as $z \to 0$:

$$\sigma_{rr}^{SF}(a,0) = \sigma_0 \left(\nu - \frac{1}{2} \right) \tag{5}$$

$$\sigma_{zz}^{SF}(a,0) = \frac{\sigma_0}{2} \tag{6}$$

$$\sigma_{rz}^{SF}(a,0) = -\frac{\sigma_0}{\pi}. \tag{7}$$

After assembling the shrink-fit, a point force P is applied acting into the elastic half-space. In the cylindrical coordinate set of Figure 1, the state of stress within the half-space is given by Timoshenko [3], and the tractions arising on any cylindrical cut (an $r =$ constant surface), $\sigma_{ij}^P(r,z)$ are given by

$$\sigma_{rr}^P(r,z) = \frac{P}{2\,\pi} \left\{ (1-2\,\nu) \left[\frac{1}{r^2} - \frac{z}{r^2\,(r^2+z^2)^{1/2}} - \frac{3\,r^2\,z}{(r^2+z^2)^{5/2}} \right] \right\} \tag{8}$$

$$\sigma_{zz}^P(r,z) = -\frac{3\,P}{2\,\pi} \left\{ \frac{z^3}{(r^2+z^2)^{5/2}} \right\} \tag{9}$$

$$\sigma_{rz}^P(r,z) = -\frac{3\,P}{2\,\pi} \left\{ \frac{r\,z^2}{(r^2+z^2)^{5/2}} \right\}. \tag{10}$$

Considering a fully stuck solution, the stresses $\tilde{\sigma}_{ij}(r,z)$ for the bilateral solution can be obtained as a sum of the shrink-fit stresses (eqs. (2) to (4)) and the tractions due to the application of the load P (eqs. (8) to (10)):

$$\tilde{\sigma}_{rr}(r,z) = \sigma_{rr}^{SF}(r,z) + \sigma_{rr}^P(r,z) \tag{11}$$

$$\tilde{\sigma}_{zz}(r,z) = \sigma_{zz}^{SF}(r,z) + \sigma_{zz}^P(r,z) \tag{12}$$

$$\tilde{\sigma}_{rz}(r,z) = \sigma_{rz}^{SF}(r,z) + \sigma_{rz}^P(r,z). \tag{13}$$

Figure 2 shows the radial normal stress ($\tilde{\sigma}_{rr}(a,z)$), the shear stress ($\tilde{\sigma}_{rz}(a,z)$) and the ratio between those at the shaft-hole interface ($r = a$). The stresses are normalised by the the reference axial stress σ_0. A normalised variable λ is chosen as a measurement of the shrink-fit to applied load stress ratio, given by

$$\lambda = \frac{P}{a^2\,\sigma_0}. \tag{14}$$

Therefore, $\lambda = 0$ represents the contact assembly, i.e. only the shrink-fit stresses are present. A positive λ implies that the shaft is being 'pushed in', towards the core of the half-space, while $\lambda < 0$ represents the shaft being 'pulled out', towards the exterior of the half-space.

Analysing the radial stress (Figure 2 (a)), we notice that as we push the shaft in ($\lambda > 0$), σ_{rr} is compressive and increases in absolute value inside the contact interface (underneath the surface). However, at the surface, as λ increases, the radial stress decreases in absolute value until it reaches zero for $\lambda = 3.1$, which would indicate contact separation at the surface. As we pull the shaft out ($\lambda < 0$), σ_{rr} is still compressive but increases in absolute value at the surface as the load P is increased. Beneath the surface, as λ increases in absolute value, the radial stress decreases until it reaches zero for $\lambda = -2.9$, which would indicate sub-surface contact separation.

Now, looking at the shear to normal stress ratio (Figure 2 (c)), we notice that for a realistic coefficient of friction ($0 \le f \le 1$) the slip condition is violated even on assembly. For instance, if $\lambda = 0$, a coefficient of friction of 1.6 would be required to guarantee that the shaft-hole interface does not slip. Therefore, the assumption of a fully

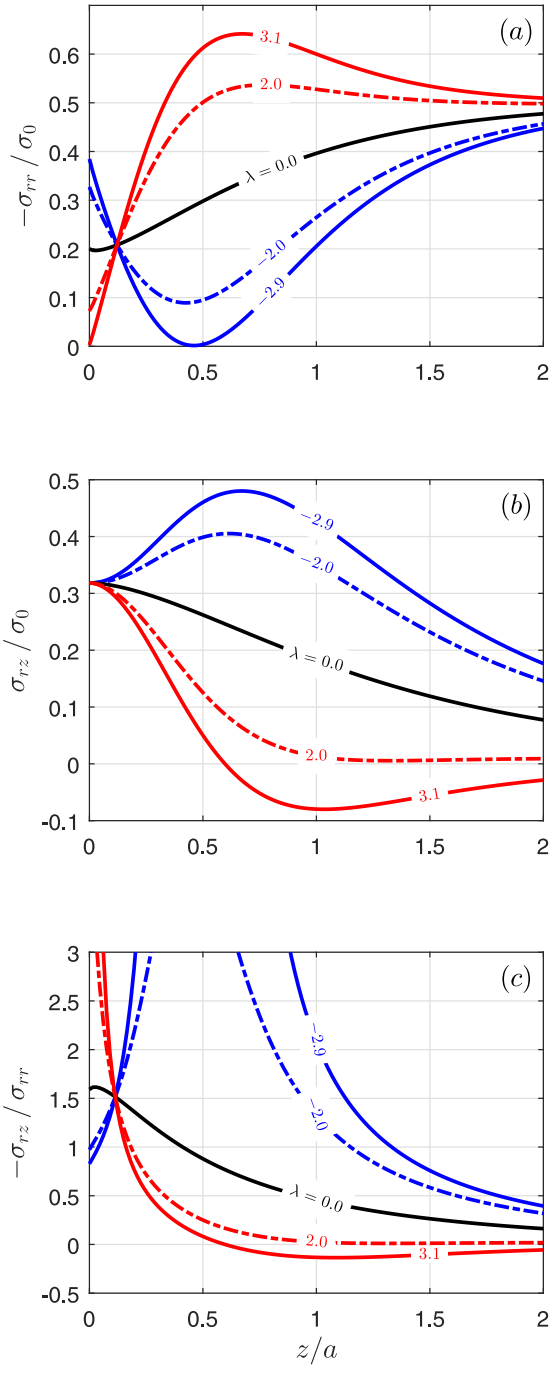

Figure 2: Stresses at the interface radius ($r = a$) versus depth z/a for varying λ. Adhered solution: (a) pressure, (b) shear and (c) traction ratio.

stuck contact interface does not hold. Slip would penetrate from the surface to a self determining point c. The traction ratio $-\sigma_{rz}/\sigma_{rr}$ increases even further in value as the force P is applied, at the surface if $\lambda > 0$ and subsurface if $\lambda < 0$.

3. Formulation

The general principle in obtaining a solution will be to develop expressions for the tractions on the shaft-hole interface, $N(z), S(z)$, representing the normal and shear components, respectively, as the sum of the bilateral solutions together with an integral representation of slip in the form of a distribution of glide dislocations. The dislocations needed are all 'edge' in character, with their Burgers vectors lying in a $\theta = constant$ plane. Only glide dislocations are needed in this problem.

A $b_z(\xi)$ dislocation loop, of radius a and with the dislocation lying at a depth ξ may be formed by making a path cut along the cylinder $r = a$ between the dislocation and the free surface of the half-space and sliding the outer wall with respect to the inner wall by a constant amount b_z. This generates a glide dislocation which is of the Volterra kind (path-cut independent) and will be used to represent slip displacement. It will induce tractions along the same cylinder $\bar{\sigma}_{zi}(z)$, where $i = r, z$, given by

$$\bar{\sigma}_{zi}(z) = G^z_{zi}(z, \xi) b_z(\xi). \tag{15}$$

The functions $G^z_{zi}(z, \xi)$ are extremely complicated in form and are defined for an isotropic half-space in [4], as well as being explicitly provided in Appendix A and as a supplementary material in [5]. They are bounded ('regular') when $i = z$ but display a Cauchy singularity when $i = r$.

3.1. Pulling the shaft out

We first look at the problem where the shaft is being 'pulled out' ($\lambda < 0$). In this case, the resulting tractions on the plane of the shaft-hole interface are given by

$$N(z) = \tilde{\sigma}_{rr}(z) + \int_{slip} G^z_{rr}(z, \xi)\, B_z(\xi) \mathrm{d}\xi \tag{16}$$

$$S(z) = \tilde{\sigma}_{rz}(z) + \int_{slip} G^z_{rz}(z, \xi)\, B_z(\xi) \mathrm{d}\xi \tag{17}$$

where $B_i(\xi) = db_i/d\xi$, $i = r, z$. Glide dislocations are installed over the interface region where slipping occurs.

The condition of slip states that the shear traction is limited by normal traction at the contact interface, giving, if the bilateral shear traction is positive,

$$N(z) < 0 \tag{18}$$

$$S(z) = -f\, N(z) \qquad 0 \le z \le c \tag{19}$$

where f is the coefficient of friction between the shaft and the hole, and c the depth to which slip penetrates.

The boundary conditions in eqs. (18) and (19) together with eqs. (16) and (17) define the following Cauchy integral equation

$$\int_0^c \left[G^z_{rz}(z,\xi) + f\, G^z_{rr}(z,\xi)\right]\, B_z(\xi)\mathrm{d}\xi = - \left[\tilde{\sigma}_{rz}(z) + f\tilde{\sigma}_{rr}(z)\right] \qquad 0 \le z \le c. \tag{20}$$

This equation possesses the property that the range of the integrals is the same as the range of imposition of the right hand side, so that it constitutes a well-posed integral equation with a generalized Cauchy kernel. It must be solved numerically using a standard numerical quadrature devised by Erdogan et al. [6].

First, we put it in standard form over the interval $[-1\,,1]$ utilising the substitutions

$$s = \frac{2\,\xi}{c} - 1\,, \qquad t = \frac{2\,z}{c} - 1 \qquad 0 \le z, \xi \le c \tag{21}$$

which give

$$\int_{-1}^{1} \left[G^z_{rz}(t,s) + f\, G^z_{rr}(t,s)\right]\, B_z(s)\mathrm{d}s = - \left[\tilde{\sigma}_{rz}(t) + f\,\tilde{\sigma}_{rr}(t)\right]. \tag{22}$$

Now, we must consider the general form of the solution required, noting that the displacement gradient must be square root bounded at both ends of the interval, at the surface ($t = -1$) and at the sticking point ($t = 1$). Thus, we assume a fundamental function as

$$B_z(s) = \phi_z(s)\,\sqrt{1-s^2} \tag{23}$$

$$\tag{24}$$

which leaves the unknown dislocation density being represented by the function $\phi_z(s)$.

Equation (22) can be expressed now, in normalised form, as

$$\sum_{i=1}^{N} \pi\, W_i\, \phi_z(s) \left[G^z_{rz}(s_i,t_k) + f G^z_{rr}(s_i,t_k)\right] = - \left[\tilde{\sigma}_{rz}(t_k) + f\,\tilde{\sigma}_{rr}(t_k)\right] \qquad t_k = 1,\ldots,N+1 \tag{25}$$

where the integration points s_i, collocation points t_k and weights W_i for the quadrature are given as

$$s_i = \cos\left(\pi \frac{i}{N+1}\right) \qquad i = 1,\ldots,N \tag{26}$$

$$t_k = \cos\left(\frac{\pi}{2}\frac{2k-1}{(N+1)}\right) \qquad i = 1,\ldots,N+1 \tag{27}$$

$$W_i = \frac{1-s_i^2}{2\,(N+1)}. \tag{28}$$

From eq. (25), we have a set of $N+1$ equations for $N+1$ unknowns. These are the N values of $\phi_z(s_i)$ and the stick point c. Once ϕ_z is known, the stresses at a point (r,z) can be found as

$$\sigma_{ij}(r,z) = \sigma_{ij}(r,z) + \int_0^c G^z_{ij}(r,z,\xi)\, B_z(\xi)\mathrm{d}\xi \qquad i,j = r,z. \tag{29}$$

3.2. Pushing the shaft in

When the shaft is pushed towards the core of the half space ($\lambda > 0$), there is further forward slip at the interface, extending from the surface to a self-determining point b ($b < c$). The set of dislocations used before is not sufficient to correct the additional slip. This requires the imposition of a new set of dislocations at the shaft-hole interface inside the slip zone.

The resulting tractions on the plane of the shaft-hole interface are now given by

$$N(z) = \tilde{\sigma}_{rr}(z) + \int_{initial\ slip} G^z_{rr}(z,\xi)\, B_z(\xi)\mathrm{d}\xi + \int_{slip} G^z_{rr}(z,\xi)\, B_z(\xi)\mathrm{d}\xi \tag{30}$$

$$S(z) = \tilde{\sigma}_{rz}(z) + \int_{initial\ slip} G^z_{rz}(z,\xi)\, B_z(\xi)\mathrm{d}\xi + \int_{slip} G^z_{rz}(z,\xi)\, B_z(\xi)\mathrm{d}\xi. \tag{31}$$

The boundary conditions remain those in eqs. (18) and (19), that together with eqs. (30) and (31) define the following Cauchy integral equation

$$\int_0^c \left[G^z_{rz}(z,\xi) + f\, G^z_{rr}(z,\xi)\right]\, B_z(\xi)\mathrm{d}\xi + \int_0^b \left[G^z_{rz}(z,\xi) + f\, G^z_{rr}(z,\xi)\right]\, B_z(\xi)\mathrm{d}\xi = - \left[\tilde{\sigma}_{rz}(z) + f\,\tilde{\sigma}_{rr}(z)\right] \qquad 0 \le z \le b. \tag{32}$$

Once again, the integrals have to be put in standard form over the interval $[-1\,,1]$ utilising the substitutions

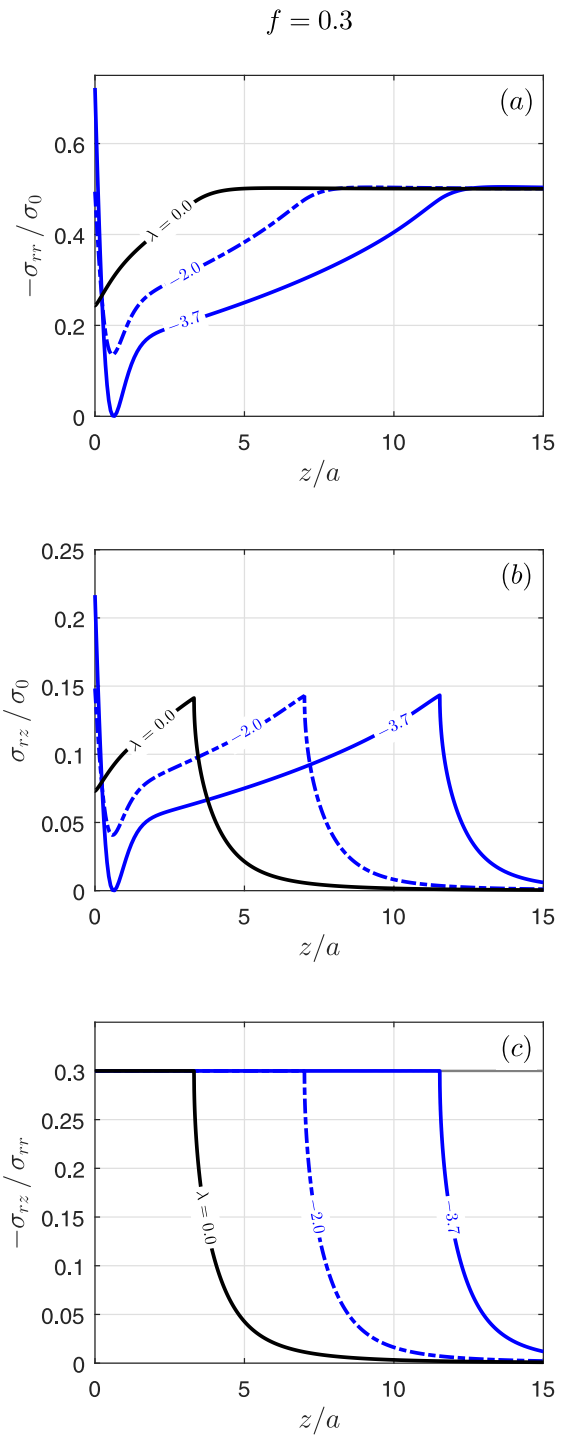

Figure 3: Stresses at the interface radius ($r = a$) versus depth z/a for $\lambda \leq 0$ and $f = 0.3$. Corrected solution: (a) pressure, (b) shear and (c) traction ratio.

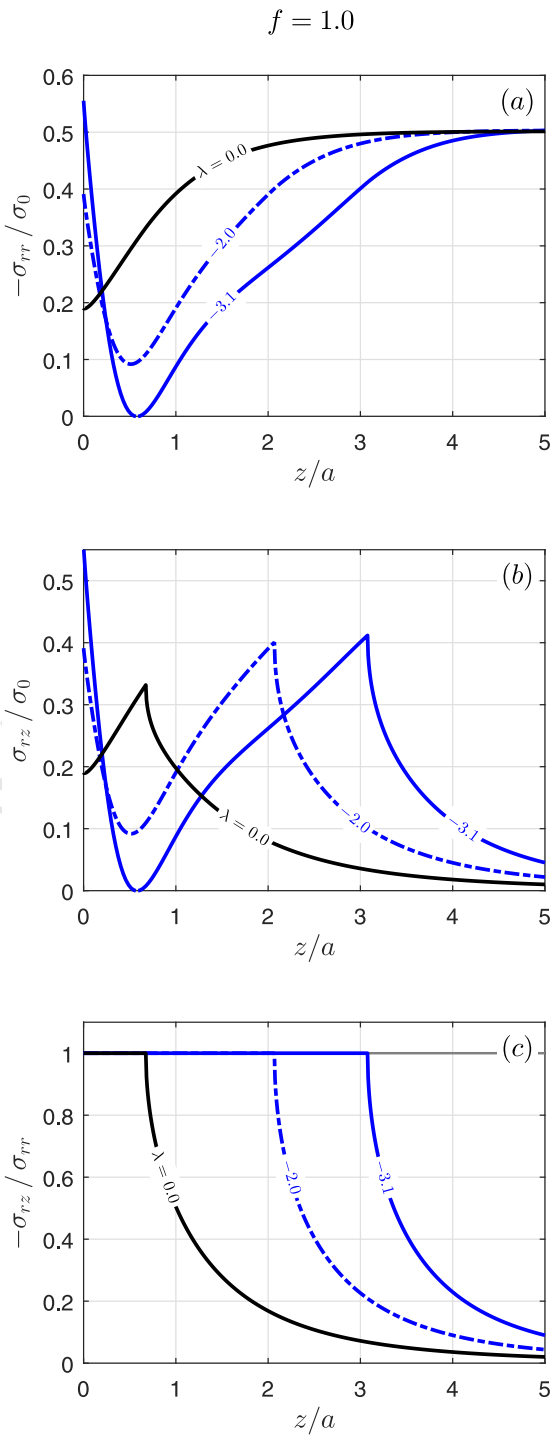

Figure 4: Stresses at the interface radius ($r = a$) versus depth z/a for $\lambda \leq 0$ and $f = 1.0$. Corrected solution: (a) pressure, (b) shear and (c) traction ratio.

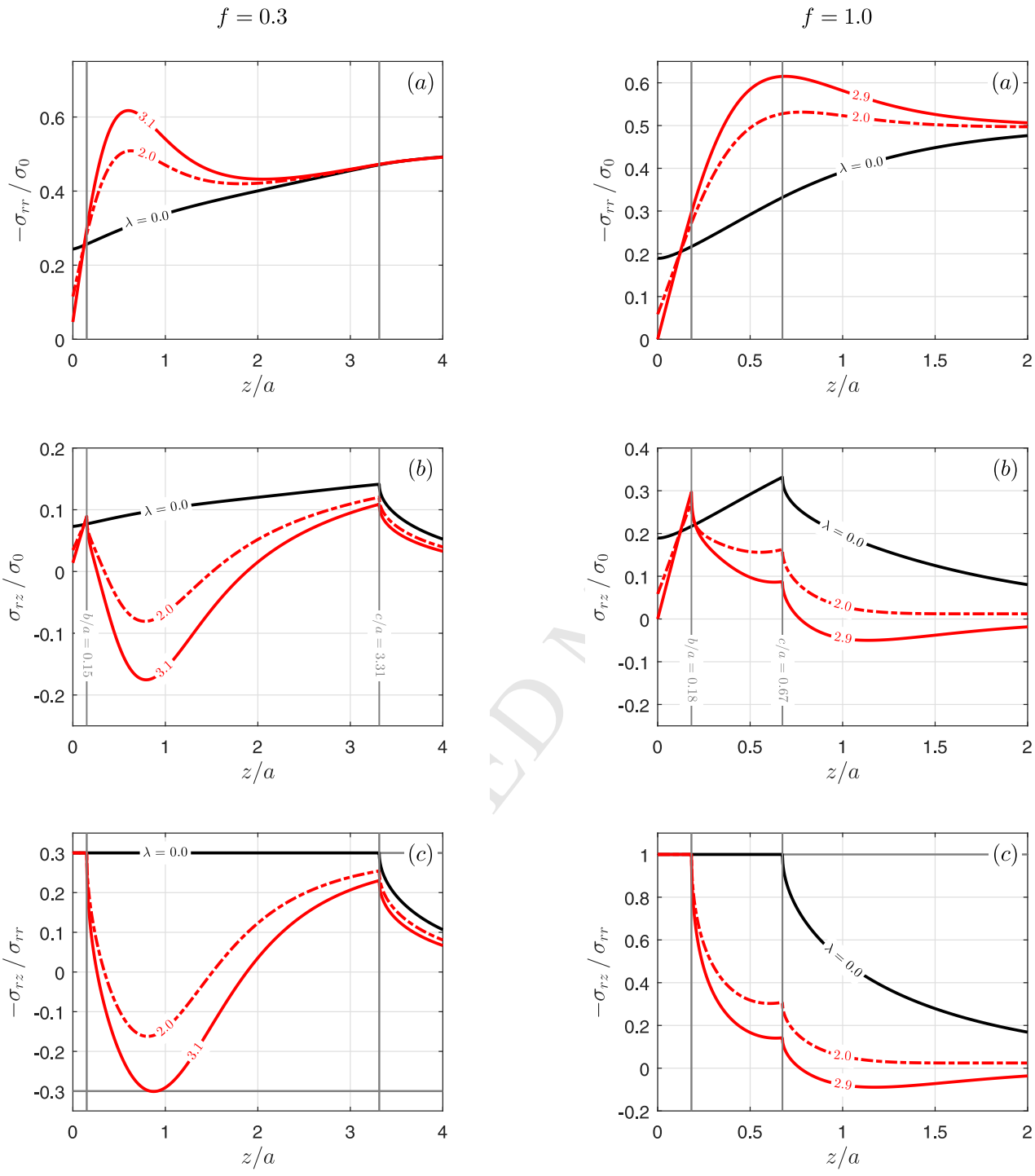

Figure 5: Stresses at the interface radius ($r = a$) versus depth z/a for $\lambda \geq 0$ and $f = 0.3$. Corrected solution: (a) pressure, (b) shear and (c) traction ratio.

Figure 6: Stresses at the interface radius ($r = a$) versus depth z/a for $\lambda \geq 0$ and $f = 1.0$. Corrected solution: (a) pressure, (b) shear and (c) traction ratio.

$$s = \frac{2\,\xi}{c} - 1\,, \qquad t = \frac{2\,z}{c} - 1 \qquad 0 \le z, \xi \le c \quad (33)$$

$$u = \frac{2\,\xi}{b} - 1\,, \qquad v = \frac{2\,z}{b} - 1 \qquad 0 \le z, \xi \le b \quad (34)$$

which give

$$\int_{-1}^{1} \left[G^z_{rz}(t,s) + f\,G^z_{rr}(t,s)\right]\, B_z(s)\mathrm{d}s + \int_{-1}^{1} \left[G^z_{rz}(v,u) + f\,G^z_{rr}(v,u)\right]\, B_z(u)\mathrm{d}u = -\left[\tilde{\sigma}_{rz}(v) + f\,\tilde{\sigma}_{rr}(v)\right]. \quad (35)$$

The displacement gradient again must be square root bounded at both ends of the interval ($v = \pm 1$) and we assume

$$B_z(u) = \psi_z(u)\,\sqrt{1-u^2}. \quad (36)$$

(37)

Equation (35) can be expressed now, in normalised form, as

$$\sum_{i=1}^{N} \pi\,W_i\,\phi_z(s)\left[G^z_{rz}(s_i,t_k) + fG^z_{rr}(s_i,t_k)\right] + \sum_{i=1}^{N} \pi\,X_i\,\psi_z(u)\left[G^z_{rz}(u_i,v_k) + fG^z_{rr}(u_i,v_k)\right] = -\left[\tilde{\sigma}_{rz}(v_k) + f\,\tilde{\sigma}_{rr}(v_k)\right] \qquad t_k = 1,\ldots,N+1 \quad (38)$$

where the integration points u_i, collocation points v_k and weights X_i for the quadrature are given as

$$u_i = \cos\left(\pi\frac{i}{N+1}\right) \qquad i = 1,\ldots,N \quad (39)$$

$$v_k = \cos\left(\frac{\pi}{2}\frac{2k-1}{(N+1)}\right) \qquad i = 1,\ldots,N+1 \quad (40)$$

$$X_i = \frac{1-u_i^2}{2\,(N+1)}. \quad (41)$$

From eq. (38), we have a set of $N+1$ equations for $N+1$ unknowns. These are the N values of $\psi_z(u_i)$ and the point b. The function $\phi_z(s_i)$ is obtained from the solution of eq. (25). Once ψ_z is known, the stresses at the bodies can be found as

$$\sigma_{ij}(r,z) = \sigma_{ij}(r,z) + \int_{-1}^{1} G^z_{ij}(t,s)\,\phi_z(s)\mathrm{d}s + \int_{-1}^{1} G^z_{ij}(v,u)\,\psi_z(u)\mathrm{d}u \qquad i,j = r,z. \quad (42)$$

4. Results

The problem was coded up using the numerical processor MATLAB. Convergence of the solution was obtained when N was set to 80. The results are for $\nu = 0.3$. In the problem, there are two length dimensions to be determined (c and b, if $\lambda > 0$) from the additional collocation equations that need to be satisfied. In practice, we guess the value of the length to be found and omit the central equation from the $N+1$ generated. The column vector of ϕ_z or ψ_z is found and the omitted equation is evaluated. The length to be found is adjusted to minimize the residue obtained from the omitted equation.

Consider first the shear stress (Figures 3 to 6 (b)). For the case where the shaft is being 'pulled out' ($\lambda < 0$) we notice that the more we 'pull the shaft out' (as λ becomes more negative), the larger the slip zone. Therefore, as we extract the shaft, the size of the slip zone increases with the magnitude of the extraction load P. When the shaft is being 'pushed in' ($\lambda > 0$) we notice that the size of the slip zone is independent of λ. As λ increases, the slip zone remains 'locked' at the assembly position (when $\lambda = 0$). To account for this effect there is additional forward slip closer to the surface ($0 \le z \le b$). For all values of λ, as the coefficient of friction f decreases, the slip zone increases, as expected. Figures 3 to 6 (a) show the contact pressure. If $\lambda < 0$ (shaft being 'pulled out'), we notice that, as the extraction force increases in magnitude, the pressure increases at the surface but decreases sub-surface. When λ reaches a critical value (-3.7 for $f = 0.3$ or -3.1 for $f = 1.0$), the contact pressure becomes null, which results in contact opening in a sub-surface point. This is in line with what was expected from the adhered solution. The ratio between the shear traction and contact pressure (Figures 3 and 4 (c)) remains positive and does not violates the slip condition as λ increases in magnitude.

If $\lambda > 0$ ('pushing the shaft in'), it is noted that as the force increases in magnitude, the pressure now increases sub-surface but decreases at the surface. For $f = 1.0$, a value of λ equal to 2.9 results in contact opening at the surface ($\sigma_{rr}(a,0) = 0$). However, for $f = 0.3$, as λ increases, the slip condition is violated before there is contact opening at the surface ($\sigma_{rz}/\sigma_{rr} > -f$). This would result in a sub-surface patch of reverse slip.

Figure 7 summarises the region where the solution is valid for a given coefficient of friction, labelled 'Forward Slip'. The blue lines represent contact opening at the surface (for $\lambda > 0$) or sub-surface (for $\lambda < 0$). The red line represent the values of λ that result in a patch of reverse slip for a given f. For $f = 0.34$ and $\lambda = 3.61$, reverse slip and contact opening happen simultaneously. For $f < 0.34$, reverse slip occurs before the contact opens at the surface.

4.1. Finite Shaft

The next step is to consider what happens if the shaft is of finite length and terminates at a depth d, by the introduction of a 'free' surface at a depth d outside the

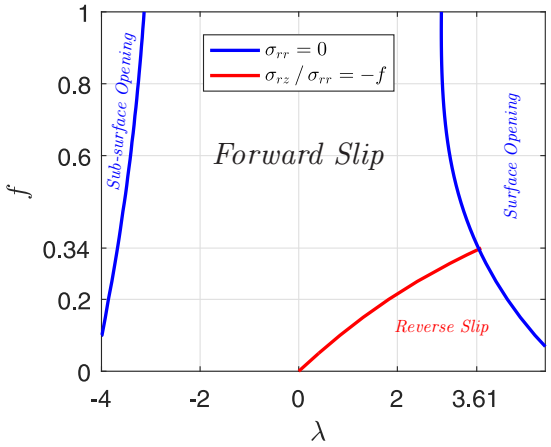

Figure 7: Values of load ratio λ required to cause contact opening or reverse slip for a given f. The solution is valid in the region marked 'Forward Slip'.

slip zone ($d > c$). Figures 8 and 9 show the stresses at a constant depth (obtained from eqs. (29) and (42)) for the two values of λ that would cause contact separation at the shaft-hole interface. From these results, we notice that, at a potential surface of depth d, the axial stress is compressive for all depths, *even if the shaft is being extracted from the hole* (Figures 8 and 9 (a)). This is due to the compressive nature of the shrink-fit assembly that results in the axial stresses due to shrink-fit being at least six times the values of axial stresses for the application of the load P, when $\lambda \sim 3$. Besides, the ratio between the shear and axial stress does not surpasses the coefficient of friction, which means that the potential surface would be stuck to the half space beneath it. Even though these results are only for $f = 1.0$, the same behaviour is observed for all values of f. Therefore, the introduction of a free surface at any depth would result in this surface being stuck to the half-space underneath it (Figure 10) and the solution found in Section 3 remains valid.

5. Conclusions

The slip present in a shrink fit, axisymmetric problem, devoid of torsion, subjected to an axial force, has been solved by using a bilateral solution for a shrink fitted shaft finishing flush with the surface of the surrounding material. Slip surfaces are represented by using arrays of axisymmetric dislocations. Conventional Gauss-Chebyshev quadrature is used to find their density. It was shown that, when the shaft is being 'pulled out' towards the exterior of the hub, the size of the slip zone increases with the load magnitude, but as we 'push the shaft in', towards the core of the hub, the slip zone remains locked at the assembly position. Also, the solution for a semi-infinite shaft is still valid for a finite shaft of depth d, as long as the surface extends beyond the slip zone.

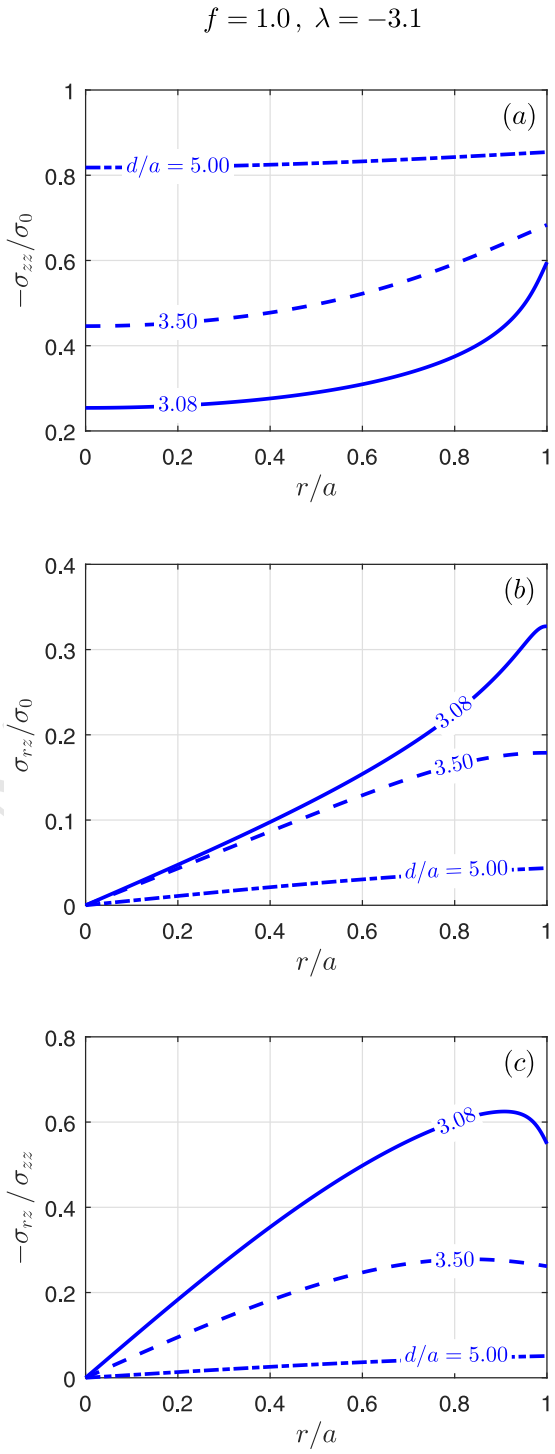

Figure 8: Stresses at a depth d/a for $f = 1.0$ and $\lambda = -3.1$: (a) axial pressure, (b) shear and (c) traction ratio.

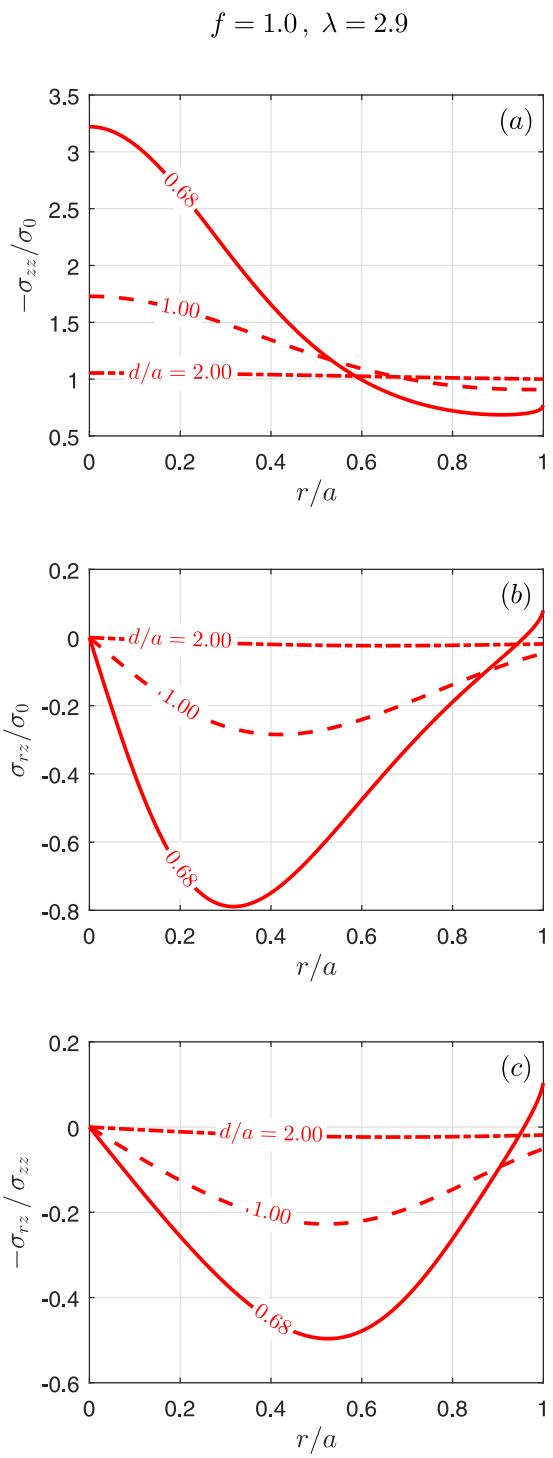

Figure 9: Stresses at a depth d/a for $f = 1.0$ and $\lambda = 2.9$: (a) axial pressure, (b) shear and (c) traction ratio.

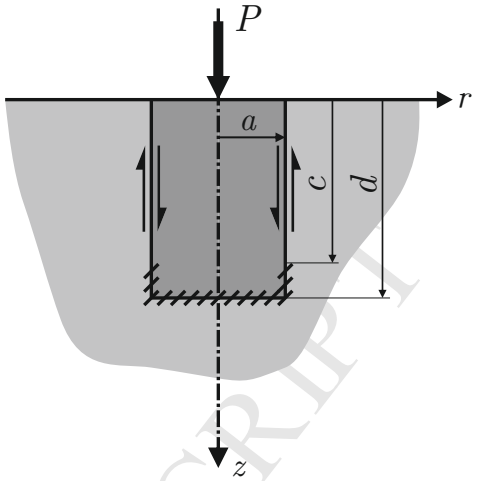

Figure 10: A finite shaft of radius a in a half-space $z > 0$.

Besides obtaining the stress fields for the shaft-hub assembly, one of the prime motivations for carrying out this calculation is to show that the glide ring dislocation is a viable quantity to use as a kernel in studying axisymmetric contact problems.

Acknowledgements

J. L. gratefully acknowledges the financial support of Christ Church Oxford, Rolls Royce PLC and CAPES [grant number 88881.128590/2016-01].

References

[1] J. R. Barber, Elasticity, Springer, 1992.
[2] R. Paynter, D. Hills, J. Barber, Features of the stress field at the surface of a flush shrink-fit shaft, Proceedings of the Institution of Mechanical Engineers, Part C: Journal of Mechanical Engineering Science 223 (10) (2009) 2241–2247. doi:10.1243/09544062JMES1403.
[3] S. Timoshenko, J. N. Goodier, Theory of Elasticity, Vol. 49, 1986. doi:10.1007/BF00046464.
[4] R. Paynter, D. Hills, The effect of path cut on Somigliana ring dislocations in a half-space, International Journal of Solids and Structures 46 (2) (2009) 412–432. doi:10.1016/j.ijsolstr.2008.09.001.
[5] J. Lopes, D. Hills, Ring cracks at the surface of a half-space, Engineering Fracfure Mechanics.
[6] F. Erdogan, G. D. Gupta, T. Cook, Numerical solution of singular integral equations, in: Methods of analysis and solutions of crack problems, 1973, pp. 368–425.
[7] G. Eason, B. Noble, I. N. Sneddon, On certain integrals of Lipschitz-Hankel type involving products of Bessel functions, Philosophical Transactions of the Royal Society of London A: Mathematical, Physical and Engineering Sciences 247 (935) (1955) 529–551.
[8] R. Paynter, D. Hills, A. Korsunsky, The effect of path cut on Somigliana ring dislocation elastic fields, International Journal of Solids and Structures 44 (2) (2007) 6653–6677. doi:10.1016/j.ijsolstr.2008.09.001.

Appendix A. State of stress induced by circular edge dislocation loops

Consider a dislocation loop put at a position (r, z) in a cylindrical coordinate system and being observed at a depth d. To calculate the influence functions, the coordinates are normalised with respect to the dislocation ring radius a:

$$\rho = r/a \qquad \zeta = z/a \qquad \delta = d/a. \tag{A.1}$$

The influence functions G^z_{zi} $(i = r, z)$ for the glide dislocation in a half-space are given as [4]:

$$\begin{aligned} G^z_{rr} = \frac{2\,\mu}{a\,(\kappa+1)} \Bigg[& - J_{1,0;1} + I_{1,0;1} + \\ & (\zeta - \delta)\, J_{1,0;2} + (\zeta - 3\,\delta)\, I_{1,0;2} + \\ & \frac{(\kappa-1)}{2\,\rho}\, J_{1,1;0} - \frac{(\kappa-1)}{2\,\rho}\, I_{1,1;0} - \\ & \frac{(\zeta-\delta)}{\rho}\, J_{1,1;1} + \frac{(\zeta\,\kappa-\delta)}{\rho}\, I_{1,1;1} + \\ & \frac{(2\,\zeta\,\delta)}{\rho}\, I_{1,1;2} - 2\,\zeta\,\delta\, I_{1,0;3} \Bigg] \end{aligned} \tag{A.2}$$

$$\begin{aligned} G^z_{rz} = \frac{2\,\mu}{a\,(\kappa+1)} \Bigg[& - (\zeta - \delta)\, J_{1,1;2} + \\ & (\zeta - \delta)\, I_{1,1;2} - 2\,\zeta\,\delta\, I_{1,1;3} \Bigg] \end{aligned} \tag{A.3}$$

Appendix A.1. Lipschitz-Hankel integrals

In the influence functions, the terms $J_{n,p;q}$ and $I_{n,p;q}$ represent Lipschitz-Hankel integrals. The standard definition for these functions is as an integral of the product of Bessel functions $(J_i(\cdot))$, an exponential term and a power term. Using normalised coordinate variables, it is given as [7]

$$P_{\mu,\nu;\lambda}(\rho,\zeta) = \int_0^\infty J_\mu(t)\, J_\nu(\rho\,t)\, e^{-\zeta\,t}\, t^\lambda\, \mathrm{d}t \tag{A.4}$$

In the kernels, the follow definition is applied:

$$J_{n,p;q} = P_{n,p;q}(\rho, \zeta - \delta) \tag{A.5}$$

$$I_{n,p;q} = P_{n,p;q}(\rho, -\zeta - \delta). \tag{A.6}$$

The Lipschitz-Hankel integrals needed in the kernels are given in [8, 4] and by Lopes and Hills [5] as a supplementary material.